

IMAGING IN X-RAY RANGES TO LOCALLY INVESTIGATE THE EFFECT OF THE TWO-CLOSE-FREQUENCY HEATING IN ECRIS PLASMAS*

R. Rácz[†], S. Biri, Z. Perduk, J. Pálinkás, Institute for Nuclear Research (Atomki), Debrecen, Hungary

E. Naselli¹, M. Mazzaglia, G. Castro, L. Celona, S. Gammino, D. Mascali, G. Torrisci, INFN-Laboratori Nazionali del Sud, Catania, Italy

A. Galatá, INFN-Laboratori Nazionali di Legnaro, Legnaro, Italy

¹also at Name of Università degli Studi di Catania, Catania, Italy

Abstract

Plasma instabilities limit the ECR Ion Sources performances in terms of flux of the extracted highly charged ions by causing beam ripple and unstable operation conditions. In a 14 GHz ECRIS (Atomki, Debrecen), the effect on the plasma instabilities in an Argon plasma at Two Close Frequencies heating scheme (the frequency gap is smaller than 1 GHz) has been explored. A special multi-diagnostic setup has been designed and implemented consisting of detectors for the simultaneous collection of plasma radio-self-emission and of high spatial resolution X-ray images in the 500 eV - 20 keV energy domain (using an X-ray pinhole camera setup). We present the comparison of plasma structural changes as observed from X-ray images in single and double-frequency operations. The latter has been particularly correlated to the confinement and velocity anisotropy, also by considering results coming from numerical simulations.

INTRODUCTION

Electron Cyclotron Resonance (ECR) Ion Sources (ECRIS) are used to produce highly charged plasmas and ion beams [1]. The ion beams are usually injected into to a high energy accelerator to provide high energy ions mainly for nuclear and particle physics experiments. Demand from the users were strongly motivating the improvement and development of ion source performances since the appearance of the pioneer ECRISs.

To produce highly charged ions hot plasma should be generated. Due to the magnetic confinement of the charged particles the velocity distribution of the energetic electrons is strongly anisotropic in the plasma. This anisotropy can cause plasma kinetic instability [2] limiting the energy content of the plasma and therefore the number of the extracted highly charged ions.

Appearance threshold of the kinetic instability was investigated intensively. Strong correlation between the magnetic field configuration of the source and the onset of the instability was found [3]. The instability always raises when the B_{\min}/B_{ECR} exceeds a value around 0.8 (where B_{\min} and B_{ECR} are the minimum magnetic field and the resonant

magnetic field, respectively). This value slightly varies with the other operation conditions of the ion source (gas pressure, microwave power). Recent study [4] shown that the spectral temperature of the plasma is increasing monotonically toward the threshold value and then saturates. Energy content of the plasma cannot be increased anymore, the electrons losses caused by the unstable condition dominates the plasma processes.

Several experiments demonstrated that the plasma stability and therefore the ion beam stability can be improved by applying two frequency heating of the plasma. Both two far (resulting in two well separated ECR heating zones) and two close (frequency gap is comparable with the scale-length of the resonance) frequency heating were investigated [5, 6].

While the beneficial effect of the multiple frequency heating is proved [7] the mechanism and the dynamics of the processes caused by the second frequency are still not fully known. Therefore, we have investigated the effect on the plasma instabilities in an Argon plasma at Two Close Frequencies Heating (TCFH) scheme using two diagnostic tools; a two-pins RF probe connected to a spectrum analyzer (SA) and an X-ray pinhole camera.

Parameters of the radiofrequency spectra (obtained by the RF probe) can be used as an indication of stable and unstable plasma conditions and a quantitative estimation of the strength of the instability can be done [6].

The high spatial resolution X-ray images (taken by the pinhole camera) are used to monitor the structural changes of the plasma when the second frequency is injected.

Furthermore, numerical simulation to investigate the velocity distribution of the plasma electrons were done to interpret the complex information obtained by the help of the two diagnostic tools.

EXPERIMENTAL SETUP

Argon plasma were generated by the 14 GHz, room temperature Atomki ECRIS [8]. The B-minimum trap consists of two room temperature coils and of a NdFeB permanent magnet hexapole. The radial magnetic field measured at the plasma chamber wall is about 1.1 Tesla while the axial magnetic peak fields along the axes of the plasma chamber are 1.26 T at the injection side and 0.95 T at the extraction side. The minimum value (B_{\min}) is 0.39 T.

* Work supported by the 3th Nat. Comm. of INFN, under the Grant PAN-DORA_Gr3, for the financial support and has received funding from the European Union's Horizon 2020 research and innovation program under grant agreement No 654002 (ENSAR2-MIDAS).

[†] rracz@atomki.hu

Content from this work may be used under the terms of the CC BY 3.0 licence (© 2019). Any distribution of this work must maintain attribution to the author(s), title of the work, publisher, and DOI

The plasmas were heated by single and double frequency mode. The first 14.25 GHz signal was amplified by a klystron while the second tuneable one was provided by a TWT Amplifier operating in 13.6 GHz - 14.6 GHz frequency range. Microwaves were launched through only one waveguide by mixing the two RF signals before the plasma chamber by a power combiner. Both the forwarded and the reflected powers were measured at the closest possible point to the plasma chamber.

Schematic drawing of the experimental setup can be seen in Fig. 1.

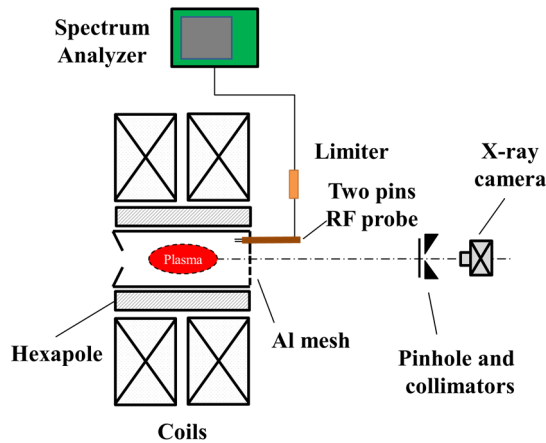


Figure 1. Drawing of the experimental setup with the two diagnostics tools.

The injection plate of the plasma chamber was adapted to the X-ray imaging: the area of the Al made circle shape injection plate was divided into two regions in the ratio 2:1. The smaller area was used for microwave and gas injection, furthermore to insert the RF-probe directly inside the plasma chamber. The larger part was closed by an Al mesh to form closed resonant cavity and to provide transparency for X-ray imaging at same time.

The X-ray pin-hole camera for 2D space resolved spectroscopy [9], consisting in a CCD camera and a lead pin-hole. The CCD camera is made of 1024 x 1024 pixels and sensitive the range 500 eV - 20 keV. It was coupled to a Pb pin-hole (thickness 2 mm, diameter $\Phi = 400 \mu\text{m}$) and placed along the axis, facing the chamber from the injection flange. A Titanium window with 9.5 μm thickness was used to screen the CCD from the visible and UV light coming out from the plasma. A multi-disks (disks with the same thickness and different hole diameter) lead collimator [10] was used as extra shielding, developed to acquire X-ray picture at up to 200 W of total incident power with appropriate signal over noise ratios. The magnification of the imaging system was 0.244.

A two-pins RF probe was connected to a Spectrum Analyser (SA) in order to detect the plasma emitted EM waves in GHz ranges characteristics of the kinetics instabilities. The flexible two-pins RF probe has an outer diameter of 4mm and a pin length of 3.5 mm. The pin distance is 2 mm. The Spectrum Analyser is operated in the range 13-15 GHz. The resolution bandwidth was 3 MHz with a sweeping time of 400 ms.

ANIZOTROPY VS. $B_{\text{MIN}}/B_{\text{ECR}}$

We have performed simulation of plasma electrons in the magnetic trap of the Atomki ECRIS under ECR conditions in single frequency heating (SFH) mode to investigate the effect of the $B_{\text{min}}/B_{\text{ECR}}$ to the anisotropy of the plasma electrons by changing the resonant frequency (consequently the resonant field). The simulation was done by TrapCAD [11, 12], which is a numerical code using a single electron approach neglecting the particle-particle interactions. The electron heating using the electron-cyclotron-resonance process is calculated by assuming a simple RF field but using realistic magnetic field configuration. A circularly polarized plane wave is assumed propagating along the z-axis. The electric vector of this type of wave is rotating in the x-y plane of the chamber. A 4th-order Runge-Kutta method is applied for the integration of the magnetic field line equation. The Lorentz force integration is processed by a time-centered leapfrog scheme explicitly solving the motion equations. The time-step of the code was set to be 3ps.

SFH mode was modelled by running the code for 15 configurations. The RF frequency was scanned from 11 GHz to 18 GHz with 500 MHz steps. The corresponding ratio $B_{\text{min}}/B_{\text{ECR}}$ is increasing from 0.6 to 0.99 by changing the frequency from 18 GHz to 11 GHz. 100,000 electrons were started from the resonant zone with 5.5 eV initial average kinetic energy both for parallel and perpendicular velocity components. Simulation is ended after 200 ns (i.e. after many RF cycles and thus giving the opportunity to the whole simulated electron bunch to interact with the wave), while the RF power was set to 200W which corresponds to 134 V/cm electrical field in the given cylindrical ECRIS plasma chamber.

Figure 2 shows the average kinetic energy of the electrons related to the parallel and the perpendicular components. The “anisotropy parameter” has been then calculated as the ratio of the average kinetic energy corresponding to the parallel and perpendicular velocity component of the electron: $An = \langle E_{\parallel} \rangle / \langle E_{\perp} \rangle$. Dependence of “An” as function of the $B_{\text{min}}/B_{\text{ECR}}$ is plotted in Fig. 3.

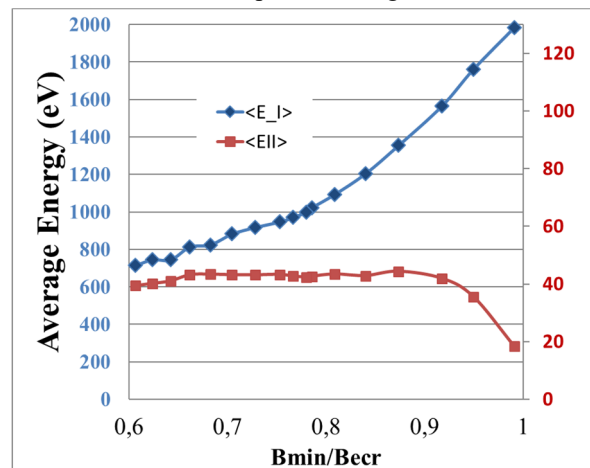


Figure 2. Average Energy of the parallel (E_{\parallel}) and the perpendicular (E_{\perp}) velocity components of the non lost electrons.

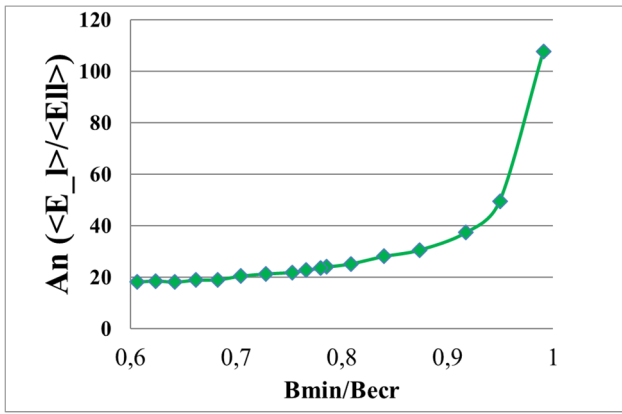


Figure 3. Dependence of the anisotropy parameter.

This plot underlines the escalation of the anisotropy toward higher B_{\min}/B_{ECR} ratios. The escalation starts close to the experimentally observed 0.8 threshold value and rapidly rises above 0.95. In the next section we will compare the anisotropy changes effected by the second frequency with the experimental results obtained by the X-ray camera and RF diagnostic system.

RESULTS AND DISCUSSION

We were taking series of X-ray images and RF spectra in single and in two frequency operation mode. In single frequency operation mode the frequency was swept from 13.6 GHz to 14.6 GHz with 50 MHz frequency steps at fixed incident microwave power (200 W). At two close frequency operation the microwave power provided by the TWT was fixed at 120 W (also in this case the frequency was swept from 13.6 GHz to 14.6 GHz with 50 MHz frequency steps) while the power launched by the fixed frequency klystron was always 80 W.

Plasma-self Emitted RF Spectra

In stable plasma conditions cases the observed frequency spectra typically show the pumping RF peak(s) only. However, in unstable plasma cases the spectra characterized by high number of plasma self-emitted sub-harmonics. By considering the number and the intensity of the sub-harmonic peaks a quantitative parameter estimating the instability strength (I_s) can be calculated [6]. In the paper [6] we demonstrated that the TCFH regime is able to dump the instabilities: it was possible to observe that the instability strength drops dramatically by adding the second pumping wave, see Fig. 4.

We have also shown that the spectral structure of the self-emitted radiation (subharmonics are detected along with the main frequencies) in TCFH mode always follows an empirical law; every time, the emission has been observed to occur at frequencies lower than the lowest of the two pumping frequencies. As an example, we present two SA spectra recorded at single frequency (13.9 GHz and 14.25 GHz) and one spectra recorded at 14.25 GHz + 13.9 GHz in double frequency heating mode (in all three cases the total net power was 200 W): they are shown, respectively, in the sequence of plots of Fig. 5. This tendency

indicates that the plasma density distribution is rearranged at TCFH mode, becoming denser in the central region of the plasma chamber (where the B-field is lower).

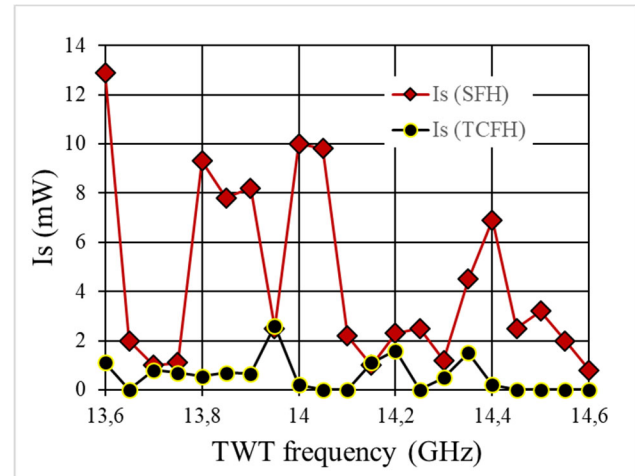


Figure 4. Instability strength as function of the applied frequency in single and in two frequency operation mode.

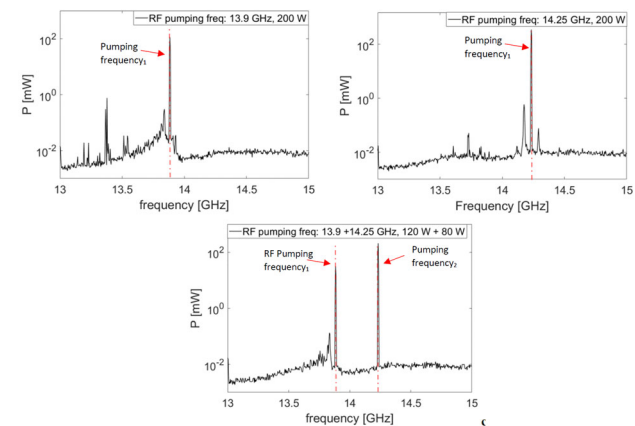


Figure 5. RF spectra measured by the spectrum analyser corresponding to single (13.9 and 14.25 GHz, at 200W) and to double frequency heating (13.9 GHz +14.25 GHz, 120 W + 80 W) operation mode.

Plasma Images

X-ray images of the plasma were taken with long (50 seconds) exposure time, while the read-out rate was 1 MHz. The Analogue Digital Unit (ADU) corresponding to every pixels and finally read by the CCD is proportional to the product of the number of incident photons and their energies. The images are able to reveal the energy content of the plasma. Figure 6. shows a typical plasma images. We can identify several distinctive areas in the image containing information about the Argon plasma, the losses of the electrons on the plasma electrode and on the cylindrical plasma chamber wall. In order to directly observe the structural changes of the plasma we have selected several ROIs (Regions of Interest) corresponding to different radial positions of the plasma. ROI-Hole gives information about the energy content of the plasma centre, while the ROI-Side characterizes the side areas of the plasmoid.

Content from this work may be used under the terms of the CC BY 3.0 licence (© 2019). Any distribution of this work must maintain attribution to the author(s), title of the work, publisher, and DOI

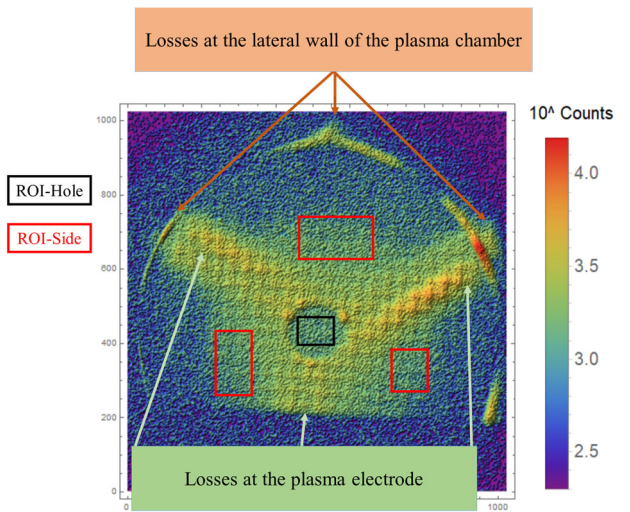


Figure 6. Typical plasma image (in logarithm scale) taken of Argon plasma generated at 13.9 GHz (single frequency mode), 200W. The exposure time was 50s.

We defined a parameter corresponding to every individual image to describe the degree of the concentration of the plasma in the central region of the chamber. This parameter is calculated as the ratio of the (area normalized) ROI-Hole (black rectangle in Fig. 6) counts of the central region and ROI-Side (red rectangle in Fig. 6) counts as the side regions of the plasma.

The higher this ratio, the plasma is more centralized. We have calculated this parameter both for single and double frequency scans and we have compared them at those frequencies where the instability was pronounced (i.e. I_s parameter is higher than 7 mW) at single frequency operation mode. These frequencies are 13.6 GHz, 13.8 GHz, 13.85 GHz, 13.9 GHz, 14 GHz, 14.05 GHz. The corresponding centralization parameters are plotted in Fig. 7. This figure together with Fig. 4 clearly demonstrate that at two close frequency heating mode the instability is effectively damped by the second frequency, meanwhile the plasma is rearranged to be denser in a central region of the plasma. This observation is in good agreement with the tendency obtained from the RF spectra, presented in Fig. 5.

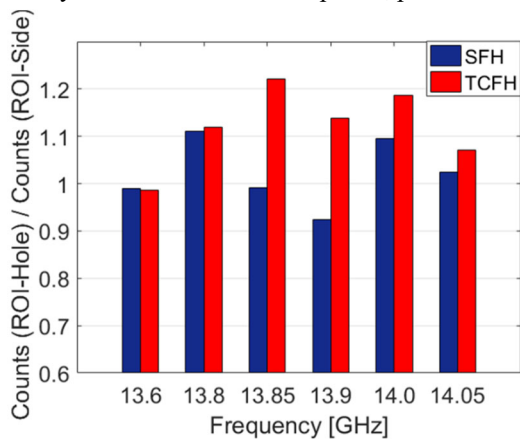


Figure 7. Centralization parameters at single and two frequency operation mode.

Comparison with Simulation Results

The effect of the second frequency to the anisotropy was investigated by the simulation code and compared with the experimentally obtained I_s parameters and the centralization parameters. Figure 8 shows these parameters in single and in double frequency operation modes (combination of 13.9 and 14.25 GHz). Each blue bar of the histogram represents the normalized anisotropy. The red curve is the experimentally measured I_s parameter, the grey bars indicate the centralization parameter, while the green rectangles report the average energy of the electrons in each simulated configuration. It can be seen that, in addition to the three experimentally investigated working point, we simulated also other two conditions in which the RF power of the two waves used for TCFH has been increased with respect to the experimental case. This plot shows that: at the same net power cases the anisotropy and the average energy decrease when we apply two close frequencies (in the simulation) and the plasma becomes more centralized meanwhile the instability is damped effectively. The additional simulated points when the TrapCAD runs in TCFH at higher total net powers, by increasing the power for both frequencies in parallel, showing that it is in principle possible to increase the average energy of the electrons (even above the energy corresponding to 13.9 GHz) and maintain anyway the anisotropy at low level.

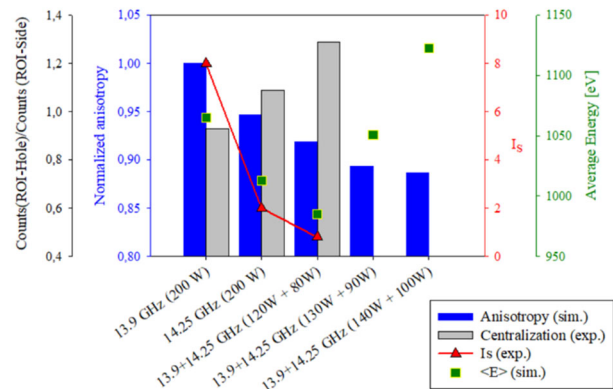


Figure 8. Comparison of simulation (sim.) and the experimental (exp.) results.

SUMMARY

We have presented experimental and simulation results corresponding to stable and unstable plasmas heated in single and two close frequency heating schemes. Non-linear increase of the anisotropy of the simulated electrons in the velocity phase space was observed around the well-known threshold value ($B_{min}/B_{ECR} \sim 0.8$) at single frequency. Instability strength and the anisotropy is moderated by applying two close frequency heating. It was also shown that when the instability is effectively damped by the second frequency the structure of the plasma is changes remarkably, the plasma becomes more centralized. One can conclude that the TCFH is making the parameter space broader and improving the plasma confinement allowing to extend the

operation conditions (using a higher amount of RF power) at B_{\min}/B_{ECR} values that are impeded by the onset of strong plasma instabilities at single frequency heating.

REFERENCES

- [1] R. Geller, "Electron Cyclotron Resonance Ion Sources and ECR Plasmas," *Institute of Physics Publishing*, Bristol, 1996.
- [2] S. V. Golubev and A. G. Shalashov, "Cyclotron-Resonance Maser Driven by Magnetic Compression of Rarefied Plasma," *Phys. Rev. Lett.*, vol. 99, p. 205002, 2007.
- [3] O. Tarvainen, J. Laulainen, J. Komppula, R. Kronholm, T. Kalvas, H. Koivisto, I. Izotov, D. Mansfeld, and V. Skalyga, "Limitations of electron cyclotron resonance ion source performances set by kinetic plasma instabilities", *Review of Scientific Instruments*, vol. 86, p. 023301, 2015.
- [4] J. B. Li, L. X. Li, B. S. Bhaskar, V. Toivanen, O. Tarvainen, D. Hitz, L. B. Li, W. Lu, H. Koivisto, T. Thuillier, J. W. Guo, X. Z. Zhang, H. Y. Zhao, L. T. Sun and H W Zhao, "Effects of magnetic configuration on hot electrons in a minimum-B ECR plasma", *Plasma Phys. Controlled Fusion*, vol. 62, p. 095015, 2020.
- [5] V. Skalyga^{1,2}, I. Izotov¹, T. Kalvas³, H. Koivisto³, J. Komppula, R. Kronholm, J. Laulainen, D. Mansfeld and O. Tarvainen, "Suppression of cyclotron instability in Electron Cyclotron Resonance ion sources by two-frequency heating," *Physics of Plasmas*, vol. 22, p. 083509, 2015.
- [6] E. Naselli, D. Mascali, M. Mazzaglia, S. Biri, R. Rácz, J. Pálinkás, Z. Perduk, A. Galatá, G. Castro, L. Celona, S. Gammmino and G. Torrissi, "Impact of two-close-frequency heating on ECR ion source plasma radio emission and stability," *Plasma Sources Sci. Technol.*, vol. 28, p. 085021, 2019.
- [7] A. Kitagawa *et al.*, "Two-frequency Heating Technique for Stable ECR Plasma", in *Proc. 20th Int. Workshop on ECR Ion Sources (ECRIS'12)*, Sydney, Australia, Sep. 2012, paper TUXO03, pp. 10-12.
- [8] S. Biri, R. Rácz and J. Pálinkás, "Status and special features of the Atomki ECR ion source," *Rev. Sci. Instrum.*, vol. 83, p. 02A341, 2012.
- [9] R. Rácz, D. Mascali, S. Biri, C. Caliri, G. Castro, A. Galatá, S. Gammmino, L. Neri, J. Pálinkás, F. P. Romano and G. Torrissi, "Electron cyclotron resonance ion source plasma characterization by energy dispersive x-ray imaging," *Plasma Sources Sci. Technol.*, vol. 26, p. 075011, 2017.
- [10] S. Biri, R. Rácz, Z. Perduk, J. Pálinkás, E. Naselli, M. Mazzaglia, G. Torrissi, G. Castro, L. Celona, S. Gammmino, A. Galatá, F.P. Romano, C. Caliri and D. Mascali, "Innovative experimental setup for X-ray imaging to study energetic magnetized plasmas," submitted to *Journal of Instrumentation*.
- [11] J. Vamosi and S. Biri, "TrapCAD - program to model magnetic traps of charged particles," *Computer Physics Communications*, vol. 98, pp. 215-223, 1996.
- [12] S. Biri, A. Derzsi, É. Fekete, I. Iván, "The upgraded TrapCAD code," *High Energy Physics and Nuclear Physics - Chinese Edition Supplement*, vol. 31, p. 165, 2007.